Monografías Matemáticas *García de Galdeano* **35**, 229–236 (2010)

EFFICIENT SECOND-ORDER DISCRETIZATIONS FOR SEMILINEAR PARABOLIC PROBLEMS

Laura Portero, Andrés Arrarás and Juan Carlos Jorge

Abstract. This work is devoted to the efficient numerical solution of semilinear parabolic problems posed on two-dimensional domains. To this end, we first carry out a spatial semidiscretization that uses a mimetic finite difference scheme based on the support-operator method. The connection between mimetic finite difference techniques and mixed finite element methods is the key to proving second-order convergence for such a scheme. Next, we consider a splitting of the semidiscrete elliptic operator subordinate to a decomposition of the spatial domain into a set of overlapping subdomains. Within this framework, we apply a second-order linearly implicit fractional step Runge-Kutta method as the time integrator. Thus, the original problem is reduced to the solution of a set of linear systems per time step. Furthermore, such linear systems can be decomposed into a set of smaller subsystems that may be solved in parallel without iterative processing.

Keywords: Domain decomposition, linearly implicit fractional step method, mimetic finite difference method, mixed finite element method, semilinear parabolic problem.

AMS classification: 35K99, 65M12, 65Y05.

§1. Introduction

Let us consider the following semilinear parabolic initial-boundary value problem: find $\psi : \Omega \times [0,T] \to \mathbb{R}$ such that

$$\psi_t(\underline{x},t) - \operatorname{div}(K(\underline{x})\ \operatorname{grad}\ \psi) = g(t,\psi) + f(\underline{x},t), \qquad (\underline{x},t) \in \Omega \times (0,T], \tag{1a}$$

$$\psi(\underline{x},0) = \psi_0(\underline{x}), \qquad \underline{x} \in \Omega, \tag{1b}$$

$$(-K(\underline{x})\ \operatorname{grad}\ \psi) \cdot \underline{n} = 0, \qquad (\underline{x},t) \in \partial\Omega \times (0,T]. \tag{1c}$$

The spatial domain $\Omega \subseteq \mathbb{R}^2$ is assumed to be a bounded open set with boundary $\partial\Omega$ and $K \equiv K(\underline{x}) = \{k_{ij}(\underline{x})\}_{2\times 2}$ is a symmetric positive definite tensor. On the other hand, $g(t,\cdot)$ denotes a nonlinear function assumed to be Lipschitz in the second variable, $f \equiv f(\underline{x},t)$ is a sufficiently smooth source/sink term and $\underline{n}$ is the outward unit vector normal to $\partial\Omega$. If we replace (1a) by an equivalent system of first-order equations, we obtain:

$$\psi_t + \operatorname{div}\ \underline{u} = g(\psi) + f, \qquad (\underline{x},t) \in \Omega \times (0,T], \tag{2a}$$

$$\underline{u} = -K\ \operatorname{grad}\ \psi, \qquad (\underline{x},t) \in \Omega \times (0,T], \tag{2b}$$

where $\underline{u} \equiv \underline{u}(\underline{x},t)$ is a vector-valued function that we refer to as the flux.

This paper proposes a numerical approach for solving (1) which is based on the method of lines, thus combining a spatial semidiscretization with a time integration. For the first stage,

the spatial domain Ω is discretized with a logically rectangular grid composed of quadrilateral elements and, then, a mimetic finite difference (MFD) method is used to approximate problem (2), (1b) and (1c). In section 2, we briefly describe the mimetic technique in the context of semilinear parabolic problems, extending the ideas proposed in [3] for the elliptic case. Following [2], a second-order convergence result in the approximation of ψ is obtained by establishing a suitable connection between MFD methods and mixed finite element (MFE) methods in Raviart-Thomas spaces.

Next, we carry out the time integration by means of a linearly implicit fractional step Runge-Kutta (FSRK) method. For that purpose, we assume Ω to be a rectangle and suppose that tensor K is diagonal and positive definite. In this setting, we construct a sufficiently smooth partition of unity subordinate to a suitable decomposition of the spatial domain and use it to define certain splittings for both the semidiscrete operator and the source/sink term (cf. [4]). The combination of such splittings with a linearly implicit FSRK method reduces the original problem to the solution of several linear systems per internal stage that can be easily parallelized. In section 3, we introduce an FSRK time integrator proposed in [5] in order to define the totally discrete scheme and show its second-order unconditional convergence. Finally, section 4 contains a numerical test that illustrates the theoretical results surveyed in the paper.

§2. Spatial semidiscretization

2.1. The mimetic finite difference method

Let $\mathcal{T}_h$ be a partition of $\overline{\Omega}$ into convex quadrilateral elements e, where $h = \max_{e\in\mathcal{T}_h} \mathrm{diam}(e)$ is the mesh size. In this work, $\mathcal{T}_h$ is assumed to be an h^2-uniform partition, i.e., each element is an h^2-parallelogram and any two adjacent elements represent an h^2-parallelogram (see [2]).

The MFD discretization may be outlined in four stages. The first one introduces the vector spaces of semidiscrete functions for both scalar and vector unknowns. On one hand, let $\mathcal{W}^h$ be the vector space of cell-centered semidiscrete scalar functions $\Psi^h = (\Psi_1^h, \Psi_2^h, \ldots, \Psi_{N_e}^h)^T$, where N_e denotes the number of mesh elements. Here, $\Psi_i^h \equiv \Psi_i^h(t)$ is associated to the center of the i-th element e_i and provides an approximation to $\psi(\underline{x}, t)|_{e_i}$. On the other hand, we denote by $\mathcal{V}^h$ the vector space of edge-based semidiscrete vector functions $\underline{U}^h = (U_1^h, U_2^h, \ldots, U_{N_\ell}^h)^T$, where N_ℓ is the number of mesh edges. In this case, $U_i^h \equiv U_i^h(t)$ is associated to the midpoint of the i-th mesh edge ℓ_i and provides an approximation to the normal component of vector $\underline{u}(\underline{x}, t)$ at ℓ_i (i.e., $\underline{u} \cdot \underline{n}_i$, where $\underline{n}_i$ is the unit vector normal to ℓ_i). Fig. 1(a) shows the local indexing of mesh vertices r_{i_j}, mesh edges ℓ_{i_j} and corresponding normal vectors $\underline{n}_{i_j}$, whereas Fig. 1(b) represents the discrete degrees of freedom for both scalar and vector functions at element e_i.

The second stage in the MFD method is to equip the previous vector spaces with appropriate inner products. The inner product on $\mathcal{W}^h$ is given by the expression $[\Psi^h, \Phi^h]_{\mathcal{W}^h} = \sum_{i=1}^{N_e} |e_i|\, \Psi_i^h\, \Phi_i^h$, where $\Psi^h, \Phi^h \in \mathcal{W}^h$ and $|e_i|$ denotes the area of the i-th element. For $\mathcal{V}^h$, we define the inner product to be $[\underline{U}^h, \underline{V}^h]_{\mathcal{V}^h} = \frac{1}{2} \sum_{i=1}^{N_e} \sum_{j=1}^{4} |T_{i_j}|\, K_i^{-1} \underline{\mathcal{U}}_{i_j}^h \cdot \underline{\mathcal{V}}_{i_j}^h$, where $\underline{U}^h, \underline{V}^h \in \mathcal{V}^h$, $|T_{i_j}|$ is the area of the triangle with vertices $r_{i_{j-1}}$, r_{i_j} and $r_{i_{j+1}}$ (with $r_0 = r_4$ and $r_5 = r_1$) and K_i is obtained from the evaluation of K at the center of the i-th element. The corner vec-

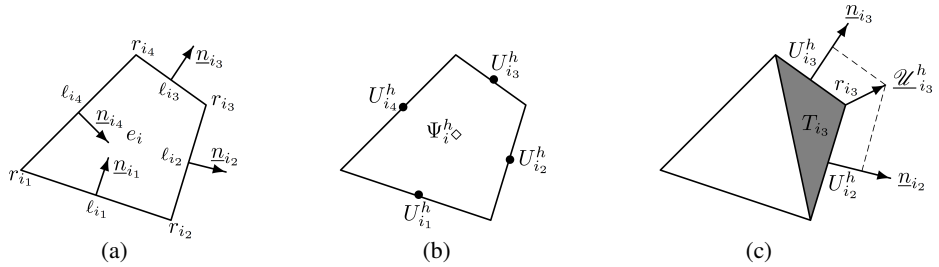

Figure 1: (a) Local indexing of vertices, edges and normal vectors at element e_i. (b) Discrete degrees of freedom for scalar and vector functions, Ψ^h and $\underline{U}^h$, at element e_i. (c) Construction of vector $\underline{\mathcal{U}}^h_{i_3}$ at vertex r_{i_3} of element e_i.

tors $\underline{\mathcal{U}}^h_{i_j}$ and $\underline{\mathcal{V}}^h_{i_j}$ are uniquely determined at the j-th vertex of e_i by using the corresponding components of $\underline{U}^h$ and $\underline{V}^h$, respectively. For instance, as displayed in Fig. 1(c), vector $\underline{\mathcal{U}}^h_{i_3}$ is obtained at node r_{i_3} as $\underline{\mathcal{U}}^h_{i_3} = U^h_{i_2}\,\underline{n}_{i_2} + U^h_{i_3}\,\underline{n}_{i_3}$, where $U^h_{i_2}$ and $U^h_{i_3}$ are those components of $\underline{U}^h$ associated with the edges ℓ_{i_2} and ℓ_{i_3}, respectively.

Once we have introduced the vector spaces of discrete functions and their corresponding inner products, the third stage in the MFD method consists of defining the discrete divergence operator, $\mathcal{D} : \mathcal{V}^h \to \mathcal{W}^h$, at the center of the i-th element, as $(\mathcal{D}\underline{U}^h)_i = |e_i|^{-1}(U^h_{i_2}\,|\ell_{i_2}| - U^h_{i_4}\,|\ell_{i_4}| + U^h_{i_3}\,|\ell_{i_3}| - U^h_{i_1}\,|\ell_{i_1}|)$, where $|\ell_{i_j}|$ denotes the length of the i-th edge, for $i = 1, 2, \ldots, N_e$ and $j = 1, 2, 3, 4$. Finally, in the fourth stage, we obtain the discrete flux operator, $\mathcal{G} : \mathcal{W}^h \to \mathcal{V}^h$, as the adjoint of $\mathcal{D}$ with respect to the inner products defined in the second stage, i.e., $\mathcal{G} = \mathcal{D}^*$ such that $[\mathcal{D}\underline{U}^h, \Psi^h]_{\mathcal{W}^h} \equiv [\underline{U}^h, \mathcal{G}\Psi^h]_{\mathcal{V}^h}$, for $\underline{U}^h \in \mathcal{V}^h$ and $\Psi^h \in \mathcal{W}^h$. This formula is a discrete version of Green's first identity. The relation of the previous inner products with the standard dot product permits us to obtain $\mathcal{G} = S^{-1}\mathcal{D}^\dagger M$, where M is a diagonal matrix given by $M = \mathrm{diag}\{|e_1|, |e_2|, \ldots, |e_{N_e}|\}$ and S is a symmetric positive-definite matrix with a 5-point stencil (cf. [3]).

The MFD method that approximates system (2), with initial and boundary data (1b) and (1c), can be written as follows: find $(\underline{U}^h, \Psi^h) : [0, T] \to \mathcal{V}^h \times \mathcal{W}^h$ such that

$$\Psi^h_t(t) + \mathcal{D}\underline{U}^h(t) = G^h(t, \Psi^h) + F^h(t), \qquad t \in (0, T], \tag{3a}$$

$$\underline{U}^h(t) = \mathcal{G}\Psi^h(t), \qquad t \in (0, T], \tag{3b}$$

$$\Psi^h(0) = \Psi^h_0, \tag{3c}$$

where vectors $G^h(t, \Psi^h)$ and $F^h(t)$ belong to $\mathcal{W}^h$ and their components are $G^h_i(t, \Psi^h) = g(t, \Psi^h_i)$ and $F^h_i(t) = |e_i|^{-1}\int_{e_i} f(\underline{x}, t)\,d\underline{x}$, respectively, for $i = 1, 2, \ldots, N_e$. Furthermore, Ψ^h_0 represents an adequate approximation to $\psi_0(\underline{x})$ to be specified later. Multiplying (3a), (3c) by $M\Phi^h$ and (3b) by $S\,\underline{V}^h$, we get, by omitting the time dependencies:

$$[\Psi^h_t, \Phi^h]_{\mathcal{W}^h} + [\mathcal{D}\underline{U}^h, \Phi^h]_{\mathcal{W}^h} = [G^h(\Psi^h), \Phi^h]_{\mathcal{W}^h} + [F^h, \Phi^h]_{\mathcal{W}^h}, \qquad \forall\, \Phi^h \in \mathcal{W}^h, \tag{4a}$$

$$[\underline{U}^h, \underline{V}^h]_{\mathcal{V}^h} = [\Psi^h, \mathcal{D}\underline{V}^h]_{\mathcal{W}^h}, \qquad \forall\, \underline{V}^h \in \mathcal{V}^h, \tag{4b}$$

$$[\Psi^h(0), \Phi^h]_{\mathcal{W}^h} = [\Psi^h_0, \Phi^h]_{\mathcal{W}^h}, \qquad \forall\, \Phi^h \in \mathcal{W}^h. \tag{4c}$$

This formulation will permit us to connect the MFD method described in the present subsection with a MFE method to be introduced next.

2.2. The mixed finite element method

Let us define $V = \left\{\underline{v} \in H(\mathrm{div};\Omega) : \underline{v}\cdot\underline{n} = 0 \text{ on } \partial\Omega\right\}$ and $W = L^2(\Omega)$, where $H(\mathrm{div};\Omega) = \{\underline{v} \in [L^2(\Omega)]^2 : \mathrm{div}\,\underline{v} \in L^2(\Omega)\}$. The variational formulation of system (2), (1b) and (1c) is: find $(\underline{u},\psi) : [0,T] \to V \times W$ such that

$$(\psi_t,\phi) + (\mathrm{div}\ \underline{u},\phi) = (g(\psi),\phi) + (f,\phi), \qquad \forall\,\phi \in W, \tag{5a}$$

$$a(\underline{u},\underline{v}) = (\psi,\mathrm{div}\ \underline{v}), \qquad \forall\,\underline{v} \in V, \tag{5b}$$

$$(\psi(0),\phi) = (\psi_0,\phi), \qquad \forall\,\phi \in W, \tag{5c}$$

where $a(\cdot,\cdot)$ is a bilinear form given by $a(\underline{u},\underline{v}) = \int_\Omega K^{-1}\,\underline{u}\cdot\underline{v}\,d\underline{x}$.

For the discretization of (5), recall that we consider an h^2-uniform partition $\mathcal{T}_h$ of $\overline{\Omega}$ consisting of convex quadrilaterals. Let $\tilde{e}$ be the reference unit square with vertices $(0,0)^T$, $(1,0)^T$, $(1,1)^T$ and $(0,1)^T$ and define a bilinear mapping $\mathcal{F}_e : \tilde{e} \to e$ which transforms the vertices of $\tilde{e}$ into the vertices of $e = \mathcal{F}_e(\tilde{e})$. If we denote by $r_i = (x_i, y_i)^T$, for $i = 1,2,3,4$, the corresponding vertices of e (counted counter-clockwise) and define $\underline{x} \equiv (x,y)$ and $\underline{\tilde{x}} \equiv (\tilde{x},\tilde{y})$, we have: $\underline{x} = \mathcal{F}_e(\underline{\tilde{x}}) = r_1(1-\tilde{x})(1-\tilde{y}) + r_2\tilde{x}(1-\tilde{y}) + r_3\tilde{x}\tilde{y} + r_4(1-\tilde{x})\tilde{y}$. We shall denote by $J_e \equiv J_e(\underline{\tilde{x}})$ and $d_e \equiv d_e(\underline{\tilde{x}})$ the Jacobian matrix of $\mathcal{F}_e$ and its determinant, respectively.

Let us now consider the lowest-order Raviart-Thomas finite element spaces on the reference element $\tilde{e}$, given by $\tilde{V}_{\tilde{e}} = Q_{1,0}(\tilde{e}) \times Q_{0,1}(\tilde{e})$ and $\tilde{W}_{\tilde{e}} = Q_{0,0}(\tilde{e})$. Here, $\tilde{V}_{\tilde{e}} \times \tilde{W}_{\tilde{e}} \subset H(\mathrm{div};\tilde{e}) \times L^2(\tilde{e})$ and $Q_{m,n}(\tilde{e})$ refers to the space of polynomial fuctions on $\tilde{e}$ of degree at most m in $\tilde{x}$ and at most n in $\tilde{y}$. The corresponding spaces $V^h \times W^h \subset V \times W$ on $\mathcal{T}_h$ are given by $V^h = \{\underline{v} \in V : \underline{v}|_e = (d_e^{-1}J_e\,\underline{\tilde{v}}) \circ \mathcal{F}_e^{-1},\ \underline{\tilde{v}} \in \tilde{V}_{\tilde{e}}\ \forall\, e \in \mathcal{T}_h\}$ and $W^h = \{\phi \in W : \phi|_e = \tilde{\phi} \circ \mathcal{F}_e^{-1},\ \tilde{\phi} \in \tilde{W}_{\tilde{e}}\ \forall\, e \in \mathcal{T}_h\}$. The so-called velocity space V^h is a finite element subspace of $H(\mathrm{div};\Omega)$ which is defined on any convex quadrilateral e via the Piola transform.

Given the finite element spaces V^h and W^h, the MFE approximation to (5) reads: find $(\underline{u}^h,\psi^h) : [0,T] \to V^h \times W^h$ such that

$$(\psi_t^h,\phi^h) + (\mathrm{div}\ \underline{u}^h,\phi^h) = (g(\psi^h),\phi^h) + (f,\phi^h), \qquad \forall\,\phi^h \in W^h, \tag{6a}$$

$$a_h(\underline{u}^h,\underline{v}^h) = (\psi^h,\mathrm{div}\ \underline{v}^h), \qquad \forall\,\underline{v}^h \in V^h, \tag{6b}$$

$$(\psi^h(0),\phi^h) = (\psi_0^h,\phi^h), \qquad \forall\,\phi^h \in W^h, \tag{6c}$$

where $g(\psi^h)$ is a piecewise constant function such that $g(\psi^h)|_{e_i} = g(\psi^h(c_i))$, being c_i the center of element e_i, and ψ_0^h denotes the elliptic mixed finite element projection of ψ_0. Finally, $a_h(\cdot,\cdot)$ is a discrete bilinear form corresponding to the application of a numerical quadrature rule for computing $a(\cdot,\cdot)$ to be defined below.

Now, we are in condition to introduce the basic tool for the error analysis of the mimetic method described in the previous subsection. Recalling the definition of the MFD vector spaces, it is possible to establish an isometry between $\mathcal{W}^h$ and W^h, given by $\mathcal{I}_{\mathcal{W}^h} : \mathcal{W}^h \to W^h$, as well as an isomorphism between $\mathcal{V}^h$ and V^h, given by $\mathcal{I}_{\mathcal{V}^h} : \mathcal{V}^h \to V^h$ (cf. [2]). Taking into account these relationships, if we compare the MFD equations (4)

with the MFE formulation (6), it is not difficult to prove that $(\operatorname{div} \underline{u}^h, \phi^h) = [\mathcal{D}\underline{U}^h, \Phi^h]_{\mathcal{W}^h}$ and $(\psi^h, \operatorname{div} \underline{v}^h) = [\Psi^h, \mathcal{D}\underline{V}^h]_{\mathcal{W}^h}$. Furthermore, the definition of Ψ^h, F^h, $G^h(\Psi^h)$ and Ψ_0^h leads to the following equalities: $(\psi_t^h, \phi^h) = [\Psi_t^h, \Phi^h]_{\mathcal{W}^h}$, $(f, \phi^h) = [F^h, \Phi^h]_{\mathcal{W}^h}$, $(g^h(\psi^h), \phi^h) = [G^h(\Psi^h), \Phi^h]_{\mathcal{W}^h}$, $(\psi_0^h, \phi^h) = [\Psi_0^h, \Phi^h]_{\mathcal{W}^h}$. Finally, the equivalence between both formulations follows from the identity $a_h(\underline{u}^h, \underline{v}^h) \equiv [\underline{U}^h, \underline{V}^h]_{\mathcal{V}^h}$. Note that the quadrature rule $a_h(\cdot,\cdot)$ provides a coercive bilinear form, thus making problem (6) be well-posed.

We refer to [1] for a detailed description of the convergence analysis for the semidiscrete scheme. The main result from that work involves the classical L^2-projection operator $\mathcal{P}_h : W \to W^h$ and may be stated as follows.

Theorem 1. *Let $\mathcal{T}_h$ be an h^2-uniform quadrilateral partition of $\overline{\Omega}$ and let $\Psi^h(t)$ denote the MFD approximation to $\psi(\underline{x}, t)$. Under sufficient smoothness and compatibility conditions on data, if we set $\psi^h(t) = \mathcal{I}_{\mathcal{W}^h}(\Psi^h(t))$ and assume that $K \in (W^{1,\infty}(e))^{2\times 2}$ and $K^{-1} \in (W^{2,\infty}(e))^{2\times 2}$ for all $e \in \mathcal{T}_h$, then there exists a constant $C > 0$, independent of h, such that $\|\mathcal{P}_h\psi(\underline{x}, t) - \psi^h(t)\| \leqslant Ch^2$ for all $t \in [0, T]$.*

2.3. Mimetic finite differences on rectangular grids

Here and henceforth, we assume that the spatial domain Ω is a rectangle $(a, b) \times (c, d)$ and $\mathcal{T}_h$ is a rectangular mesh with $N_x \times N_y$ cells whose dimensions are $h_x = (b - a)/N_x$ and $h_y = (d - c)/N_y$. Moreover, $c_{i,j} = ((i - 1/2)h_x, (j - 1/2)h_y)$ denotes the center of the (i, j)-cell $e_{i,j}$. Finally, we assume that $K(\underline{x})$ is a diagonal 2×2 tensor, whose components satisfy $k_{11}(\underline{x})$, $k_{22}(\underline{x}) > 0$ for all $\underline{x} \in \Omega$.

If we define the restriction operator to the cell centers as $r_h : L^2(\Omega) \to \mathcal{W}^h$, then it holds that $r_h|_{W^h} \equiv \mathcal{I}_{\mathcal{W}^h}^{-1}$ and $\|r_h u^h\|_h = \|u^h\|$ for all $u^h \in W^h$, where $\|U^h\|_h \equiv [U^h, U^h]_{\mathcal{W}^h}$ denotes the discrete L^2-norm associated to $\mathcal{W}^h$. Inserting (3b) into (3a), the following differential system is obtained: find $\Psi^h : [0, T] \to \mathcal{W}^h$ such that

$$\Psi_t^h(t) - \mathcal{A}\Psi^h(t) = G^h(t, \Psi^h) + F^h(t), \qquad t \in (0, T], \tag{7a}$$

$$\Psi^h(0) = \Psi_0^h, \tag{7b}$$

where $\Psi^h(t) \equiv r_h(\psi^h(t))$ and $-\mathcal{A}\Psi^h(t) \equiv \mathcal{D}(\mathcal{G}\Psi^h(t))$ is the mimetic finite difference approximation to $-\operatorname{div}(K \operatorname{grad} \psi)$. Such an approximation uses the well-known harmonic average for the elements of K in the x- and y-direction, thus leading to a standard five-cell discretization on a rectangular grid (see [3] for details).

§3. Time integration

Let us decompose Ω into the union of m overlapping subdomains $\{\Omega_\ell\}_{\ell=1}^m$, each of which consists of a certain number of disjoint connected components, i.e., $\Omega = \bigcup_{\ell=1}^m \Omega_\ell$, where $\Omega_\ell = \bigcup_{j=1}^{m_\ell} \Omega_{\ell j}$ such that $\Omega_{\ell j} \cap \Omega_{\ell k} = \emptyset$ if $j \neq k$. By considering such a decomposition, we can define a partition of unity consisting of m smooth functions $\{\rho_\ell(\underline{x})\}_{\ell=1}^m$, with $\rho_\ell : \Omega \to [0, 1]$, such that $\sum_{\ell=1}^m \rho_\ell(\underline{x}) = 1$ for all $\underline{x} \in \Omega$ and $\operatorname{supp}(\rho_\ell) \equiv \Omega_\ell$, for $\ell = 1, 2, \ldots, m$.

Next, we introduce the splittings $\mathcal{A} = \sum_{\ell=1}^{m} \mathcal{A}_\ell$ and $F^h(t) = \sum_{\ell=1}^{m} F^h_\ell(t)$, such that:

$$
\begin{aligned}
(\mathcal{A}_\ell \Psi^h)_{(i,j)} = & \frac{\rho_\ell(c_{i+1,j})\,\tilde{k}_{11}(i+1,j)\,\frac{\Psi^h_{i+1,j}-\Psi^h_{i,j}}{h_x} - \rho_\ell(c_{i,j})\,\tilde{k}_{11}(i,j)\,\frac{\Psi^h_{i,j}-\Psi^h_{i-1,j}}{h_x}}{h_x} \\
& + \frac{\rho_\ell(c_{i,j+1})\,\tilde{k}_{22}(i,j+1)\,\frac{\Psi^h_{i,j+1}-\Psi^h_{i,j}}{h_y} - \rho_\ell(c_{i,j})\,\tilde{k}_{22}(i,j)\,\frac{\Psi^h_{i,j}-\Psi^h_{i,j-1}}{h_y}}{h_y},
\end{aligned}
\tag{8}
$$

where $\tilde{k}_{11}$ and $\tilde{k}_{22}$ denote the harmonic averages of k_{11} and k_{22} in the x- and y-direction, respectively, and $(F^h_\ell(t))_{(i,j)} = \rho_\ell(c_{i,j})|e_{i,j}|^{-1} \int_{e_{i,j}} f(\underline{x},t)\,d\underline{x}$, being $|e_{i,j}|$ the area of cell $e_{i,j}$. Similar domain decomposition operator splittings have been previously used in [4]. Matrices $\{\mathcal{A}_\ell\}_{\ell=1}^m$ defined in (8) are block-tridiagonal, symmetric and non-positive definite, but they do not commute. From a theoretical point of view, this lack of commutativity requires the use of time integrators which are proven to be stable for non-commuting operators.

Following [5], let us now introduce a second-order fractional step method in order to reduce the semilinear stiff problem (7) to the solution of the following set of linear systems:

$$
\begin{cases}
\text{For } n = 0, 1, \ldots, N_T: \\
\quad \Psi^h_{n,1} = \Psi^h_n, \\
\quad \text{For } \ell = 2, 3, \ldots, 2m-1: \\
\qquad \Psi^h_{n,\ell} = \Psi^h_{n,\ell-1} + \tau \sum_{k=\ell-1}^{\ell} d_k (\mathcal{A}_{i_k} \Psi^h_{n,k} + F^h_{i_k}(t_{n,k})) + \dfrac{\tau}{2}\,\Phi^h_{n,\ell}, \\
\quad \Psi^h_{n+1} = \Psi^h_{n,2m-1},
\end{cases}
\tag{9}
$$

where $\Phi^h_{n,2} = G^h(t_{n,1}, \Psi^h_{n,1})$, $\Phi^h_{n,2m-1} = 2\,G^h(t_{n,m}, \Psi^h_{n,m}) - G^h(t_{n,1}, \Psi^h_{n,1})$ and $\Phi^h_{n,\ell} \equiv 0$, for $\ell = 3, 4, \ldots, 2m-2$. The time step is denoted by τ and $N_T \equiv [T/\tau] - 1$. Subindex i_k is such that $i_k = k$, for $k = 1, 2, \ldots, m$, and $i_k = 2m - k$, for $k = m+1, m+2, \ldots, 2m-1$. On the other hand, the intermediate times are given by $t_{n,1} = t_n = n\tau$, $t_{n,k} = t_n + \frac{\tau}{2}$, for $k = 2, 3, \ldots, 2m-2$, and $t_{n,2m-1} = t_n + \tau$, while the coefficients of the internal stages are $d_1 = d_m = d_{2m-1} = \frac{1}{2}$ and $d_j = \frac{1}{4}$, for $j \in \{2, 3, \ldots, m-1\} \cup \{m+1, m+2, \ldots, 2m-2\}$. Finally, the totally discrete solution Ψ^h_{n+1} approximates $\Psi^h(t_{n+1})$. This method, which can be seen as a linearly implicit generalization of Peaceman-Rachford fractional step method, has been proven to be stable even for non-commuting matrices $\{\mathcal{A}_\ell\}_{\ell=1}^m$ (cf. [5]).

Note that the choice of a linearly implicit scheme like (9) entails an explicit treatment of the nonlinear semidiscrete function $G^h(t, \Psi^h)$. As a consequence, at each internal stage, we have to solve a linear system with associated matrix $(\mathcal{I} - \tau\, d\, \mathcal{A}_\ell)$, where $\mathcal{I}$ is the identity matrix of order $N_x N_y$, $d > 0$ and $\ell \in \{1, 2, \ldots, m\}$. Recalling that ρ_ℓ is considered in the definition of $\mathcal{A}_\ell$ and $\operatorname{supp}(\rho_\ell) \equiv \Omega_\ell$, such a linear system involves as many unknowns as the number of cell centers lying inside Ω_ℓ. Finally, since Ω_ℓ consists of the union of several disjoint components, the linear system to solve is, in fact, a collection of several uncoupled subsystems that can be solved in parallel. It is interesting to point out that, as a difference to classical domain decomposition techniques, our proposal does not require any Schwarz iteration procedures.

To finish the section, let us define the global error of the totally discrete scheme (9) at t_{n+1} as $\|E^h_{n+1}\|_h = \|r_h(\mathcal{P}_h\psi(\underline{x}, t_{n+1})) - \Psi^h_{n+1}\|_h$. A classical combination of suitable consistency and stability properties for the time integrator, together with the bound given in Theorem 1 for the spatial semidiscretization scheme, permits us to prove the following convergence result (cf. [1]).

Theorem 2. *Let Ψ^h_{n+1} be the solution of the totally discrete scheme* (9)*. Then, there exists a constant $C > 0$, independent of h and τ, such that $\|E^h_{n+1}\|_h \leqslant C(h^2 + \tau^2)$ for all $n = 0, 1, \ldots, N_T$.*

§4. A numerical example

Let us consider the semilinear parabolic problem given by (1), where $\Omega = (0,1) \times (0,1)$, $K(\underline{x}) = (1 + x^2 + y^2)\mathcal{I}$ and $g(t,\psi) = -\frac{1}{1+\psi^2}$. Data functions f and ψ_0 are defined in such a way that $\psi(\underline{x}, t) = e^{-t}(x^2(1-x)^2 + y^2(1-y)^2)$ is the exact solution of the problem.

We consider a rectangular mesh $\mathcal{T}_h$ that covers Ω with $N_x \times N_y$ cells and we carry out the spatial semidiscretization process described in section 2. In this case, $h = \max\{\frac{1}{N_x}, \frac{1}{N_y}\}$. Then, we define $I_1 \equiv (0, \frac{5}{16}] \cup [\frac{7}{16}, \frac{13}{16}]$ and $I_2 \equiv [\frac{3}{16}, \frac{9}{16}] \cup [\frac{11}{16}, 1)$ and we set out $\Omega_1 \equiv I_1 \times I_1$, $\Omega_2 \equiv I_2 \times I_1$, $\Omega_3 \equiv I_1 \times I_2$ and $\Omega_4 \equiv I_2 \times I_2$. Thus, the spatial domain $\Omega = \bigcup_{i=1}^4 \Omega_i$ is decomposed into $m = 4$ overlapping subdomains, each of which consists of 4 disjoint connected components. In order to define a smooth partition of unity $\{\rho_\ell\}_{\ell=1}^4$, we use suitable products of dilations and translations of a C^∞ function (cf. [1]). Finally, the integral averages of f over the mesh cells are computed by using the two-dimensional Simpson's rule.

In order to test the second-order convergence of the spatial semidiscretization scheme, we consider a small fixed time step $\tau = 10^{-5}$ and, starting from a mesh with 3×4 cells, we compute the global errors resulting from doubling the number of cells in each direction. Such errors, denoted by $E_{N_x,N_y,\tau}$, are measured in the maximum norm in time and the discrete L^2-norm in space and are displayed in the upper row of Table 1. From these results, we obtain the usual estimates for the order of convergence in space as $p_{N_x,N_y,\tau} = \log_2(E_{N_x,N_y,\tau}/E_{2N_x,2N_y,\tau})$. As shown in the lower row of Table 1, $p_{N_x,N_y,\tau}$ approaches 2 when h tends to 0, as predicted in Theorem 2.

Next, we compare the numerical solution obtained for a mesh size h and a time step τ with that obtained for the same mesh size and a time step $\tau/2$ (by using again the maximum norm in time and the discrete L^2-norm in space). When considering a small enough fixed h, this quantity estimates the global error in time and can be used to check the second-order convergence of the time integrator. In this case, we consider a fine spatial grid with 96×128 cells and, starting from a time step $\tau = 10^{-1}$, we compute the global errors resulting from halving the time step. From such errors, denoted by $\bar{E}_{N_x,N_y,\tau}$, we can estimate the orders of convergence in time as $\bar{p}_{N_x,N_y,\tau} = \log_2(\bar{E}_{N_x,N_y,\tau}/\bar{E}_{N_x,N_y,\tau/2})$. Table 2 shows the values of $\bar{E}_{N_x,N_y,\tau}$ (upper row) and $\bar{p}_{N_x,N_y,\tau}$ (lower row). Observe that the numerical orders of convergence also approach 2 when τ tends to 0, as stated in Theorem 2. Finally, it is important to note that, despite the fact that the nonlinear term is treated explicitly, the method shows an unconditionally stable behaviour.

(N_x, N_y)	(3,4)	(6,8)	(12,16)	(24,32)	(48,64)	(96,128)
$E_{N_x,N_y,\tau}$	6.526E-3	2.093E-3	5.511E-4	1.395E-4	3.499E-5	8.766E-6
$p_{N_x,N_y,\tau}$	1.641	1.925	1.982	1.995	1.997	–

Table 1: Global errors and numerical orders of convergence in space ($\tau = 10^{-5}$).

τ	0.1	$0.1 \cdot 2^{-1}$	$0.1 \cdot 2^{-2}$	$0.1 \cdot 2^{-3}$	$0.1 \cdot 2^{-4}$	$0.1 \cdot 2^{-5}$
$\bar{E}_{N_x,N_y,\tau}$	8.763E-2	4.523E-2	2.224E-2	1.020E-2	4.164E-3	1.559E-3
$\bar{p}_{N_x,N_y,\tau}$	0.954	1.013	1.135	1.292	1.417	1.672
τ	$0.1 \cdot 2^{-6}$	$0.1 \cdot 2^{-7}$	$0.1 \cdot 2^{-8}$	$0.1 \cdot 2^{-9}$	$0.1 \cdot 2^{-10}$	$0.1 \cdot 2^{-11}$
$\bar{E}_{N_x,N_y,\tau}$	4.893E-4	1.424E-4	4.036E-5	1.078E-5	2.775E-6	7.012E-7
$\bar{p}_{N_x,N_y,\tau}$	1.781	1.819	1.904	1.958	1.985	–

Table 2: Global errors and numerical orders of convergence in time ($N_x = 96$, $N_y = 128$).

Acknowledgements

This work is partially supported by the Spanish Ministry of Innovation and Science under Research Project MTM2007-63772 and by Government of Navarre under Research Projects 228/2008-2301 and CTP-07/R-10.

References

[1] Arrarás, A., Portero, L., and Jorge, J. C. Convergence of fractional step mimetic finite difference discretizations for semilinear parabolic problems. *Appl. Numer. Math. 60* (2010), 473–485.

[2] Berndt, M., Lipnikov, K., Shashkov, M., Wheeler, M. F., and Yotov, I. Superconvergence of the velocity in mimetic finite difference methods on quadrilaterals. *SIAM J. Numer. Anal. 43* (2005), 1728–1749.

[3] Hyman, J., Shashkov, M., and Steinberg, S. The numerical solution of diffusion problems in strongly heterogeneous non-isotropic materials. *J. Comput. Phys. 132* (1997), 130–148.

[4] Mathew, T. P., Polyakov, P. L., Russo, G., and Wang, J. Domain decomposition operator splittings for the solution of parabolic equations. *SIAM J. Sci. Comput. 19* (1998), 912–932.

[5] Portero, L., and Jorge, J. C. A new class of second order linearly implicit fractional step methods. *J. Comput. Appl. Math. 218* (2008), 603–615.

Laura Portero, Andrés Arrarás and Juan Carlos Jorge
Departamento de Ingeniería Matemática e Informática
Universidad Pública de Navarra
Campus de Arrosadía, 31006 - Pamplona, Spain
{laura.portero,andres.arraras,jcjorge}@unavarra.es